Squaraine Rotaxanes with Boat Conformation Macrocycles

Na Fu, **Jeffrey M. Baumes**, **Easwaran Arunkumar**, **Bruce C. Noll**, and **Bradley D. Smith**[*]
Department of Chemistry and Biochemistry, University of Notre Dame, Notre Dame, IN 46545, USA

Abstract

Mechanical encapsulation of fluorescent, deep-red bis(anilino)squaraine dyes inside Leigh-type tetralactam macrocycles produces interlocked squaraine rotaxanes. The surrounding macrocycles are flexible and undergo rapid exchange of chair and boat conformations in solution. A series of X-ray crystal structures show how the rotaxane co-conformational exchange process involves simultaneous lateral oscillation of the macrocycle about the center of the encapsulated squaraine thread. Rotaxane macrocycles with 1,4-phenylene-sidewalls and 2,6-pyridine dicarboxamide bridging units are more likely to adopt boat conformations in the solid-state than analogous squaraine rotaxane systems with isophthalamide-containing macrocycles. A truncated squaraine dye, with a secondary amine attached directly to the central C_4O_2 core, is less electrophilic than the extended bis(anilino)squaraine analogue, but it is still susceptible to chemical and photochemical bleaching. Its stability is greatly enhanced when it is encapsulated as an interlocked squaraine rotaxane. An X-ray crystal structure of this truncated squaraine rotaxane shows the macrocycle in a boat conformation, and NMR studies indicate that the boat is maintained in solution. Encapsulation as a rotaxane increases the dye's brightness by a factor of six. The encapsulation process appears to constrain the dye and reduce deformation of the chromophore from planarity. This study shows how mechanical encapsulation as a rotaxane can be used as a rational design parameter to fine-tune the chemical and photochemical properties of squaraine dyes.

Introduction

Interest in mechanically interlocked molecules, especially catenanes and rotaxanes, is increasing as advances in templated synthesis allow chemists to design more complicated molecular systems with programmable functions.[1] A requirement for rational design of functional rotaxanes is a quantitative understanding of the factors that control the conformational dynamics of the mechanically bonded components.[2–4] More than a decade ago, the group of Leigh and coworkers developed a versatile rotaxane synthesis method based on a templated clipping reaction that wraps a tetralactam macrocycle around an appropriate dumbbell-shaped thread component.[5,6] Ongoing work by this group and by others have produced a spectacular array of Leigh-type rotaxanes and demonstrated sophisticated molecular functions such as shuttling, solar energy capture, and chemical sensing.[7–9] The published papers include quite a few rotaxane X-ray crystal structures, and the vast majority show the surrounding macrocycle in a chair or distorted-chair conformation.[5–7] Examples of Leigh-type rotaxanes with the tetralactam macrocycle in an obvious boat conformation are very rare.[6] However, several recent papers from different laboratories report UV and IR

spectral evidence suggesting, but not proving definitively, that the boat conformation can become favored under shuttling conditions that provide stabilizing non-covalent interactions such as aromatic stacking and hydrogen bonding.[9,10]

In 2005, we reported that the Leigh clipping methodology can be used to convert squaraine dyes, **1**, into squaraine rotaxanes, **2** (Figure 1), and we are developing squaraine rotaxanes as a new class of highly stable and very bright, deep-red fluorescent dyes.[11] We have demonstrated that the surrounding tetralactam macrocycle sterically protects the dye and greatly increases chemical stability. A more subtle question is whether the macrocycle can be used to fine-tune the squaraine photophysical properties in a controllable manner. This requires an intimate understanding of rotaxane structure and macrocycle dynamic motion. X-ray crystal structures of the first few squaraine rotaxanes that we prepared all showed the phenylene-containing tetralactam macrocycle located centrally over the squaraine dye and in a chair conformation. Here, we report a comparative study of the homologous squaraine rotaxane series, **2a–e**, and our finding of a much richer array of solid-state structures, including several examples with the surrounding macrocycle in a boat conformation. We also report the structure of a new type of truncated squaraine rotaxane, **5**, with green fluorescence, and a surrounding macrocycle that adopts a rigid boat conformation in the solid and solution-state. The reduced structural flexibility of rotaxane **5** appears to be the reason why it exhibits a significantly higher fluorescence quantum yield than its parent squaraine dye. This work expands our understanding of squaraine rotaxane dynamic structure and how it affects the photophysical properties of the encapsulated dye.

Results and Discussion

Bis(anilino)squaraine Rotaxanes

The bis(anilino)squaraine dyes **1a–d** were made by condensing the appropriate aniline precursors with squaric acid using standard literature conditions.[11] The squaraine rotaxanes **2a–e** were subsequently prepared by a common procedure that simultaneously added separate solutions of the appropriate diacid dichloride and 1,4-xylylenediamine to a solution of squaraine dye. The isolated yields for this five-component assembly process were between 26–40 % and quite reproducible.

All of the rotaxane tetralactam macrocycles in this report are comprised of two 1,4-phenylene side-walls that are connected by two identical bridging units that are either 2,6-pyridine dicarboxamide (hereafter referred to as the pyridyl-containing macrocycle) in the case of **2a–d** or isophthalamide units in **2e**. Single crystals of these five bis(anilino)squaraine rotaxanes were analyzed by X-ray diffraction, and the solved structures are illustrated in Figure 2, with the key crystallographic distances in Table 1 and associated atom labeling in Figure 3. It is worth noting that the ORTEPs of these solid-state structures show no evidence of conformational disorder (see supporting information). The structural discussion starts with the four squaraine rotaxanes, **2a–d**, that each have a pyridyl-containing macrocycle. The previously reported solid-state structure of **2a**,[11a] with R = H on the four terminal benzyl stopper groups, shows the macrocycle in a chair conformation (C_{2h} symmetry) that is commonly observed with Leigh-type rotaxanes. In striking contrast, the new crystal structures of squaraine rotaxanes **2b–d**, where R = Br, I, and CH_3, each have the surrounding pyridyl-containing macrocycle in a boat conformation (C_{2v} symmetry). Another difference is the location of the macrocycle relative to the encapsulated dye. The chair macrocycle in **2a** is located centrally and symmetrically over the core of its encapsulated squaraine, whereas the boat macrocycles in **2b–d** are translocated to one side. This co-conformation reduces the degree of cofacial overlap of the macrocycle's electron-rich 1,4-phenylene side-walls with the electron deficient C_4O_2 core of the squaraine.[12]

In an effort to rationalize this difference in solid-state conformations, we looked for diagnostic intramolecular distances that were conformation-dependent. In each structure, the macrocyclic NH residues are engaged in bifurcated hydrogen bonds with the encapsulated squaraine oxygens but there is little difference in the apparent strength of the hydrogen bonding as judged by the N•••O distances and NH•••O angles that are listed in Table 1. Similarly, the centroid-to-centroid distance between the phenylene-sidewalls in chair-conformer **2a** is 6.60 Å and quite close to the range of 6.63–6.78 Å for boat-conformers **2b–d**. As expected, the two pyridyl nitrogens, N_c and N_d, in each macrocycle form internal hydrogen bonds with the adjacent macrocycle amide NH residues.[13] In addition, the same pyridyl nitrogen atoms have short contacts with the proximal squaraine hydrogens H_a and H_b (or H_d in the case of chair-conformer rotaxane **2a**). These short, cross-component distances are indicative of an attractive interaction between dye and macrocycle but the distances are very similar for chair and boat conformations. There is a conformation-dependent difference in the cross-component distances between the pyridyl nitrogens, N_c and N_d, and squaraine oxygens, O_a and O_b; the two equal distances of 3.15 Å in symmetric chair-conformation **2a** are significantly shorter than the range of 3.21–3.50 Å for boat-conformers **2b–d**. By sliding away from the center of the dye, the boat-conformation macrocycles lowers both of these cross-component N•••O repulsions.[14] Another conformation-dependent structural difference is the shape of the encapsulated squaraine chromophore. It is planar in symmetric chair-conformer **2a** but slightly twisted and bent in boat-conformations **2b–d**. A comparative measure of this dye bending is the distance between squaraine nitrogen atoms N_a and N_b. It is 13.29 Å for the chair-conformer **2a**, which is longer than the range of 13.09–13.16 Å for boat-conformers **2b–d**. It appears that the encapsulated squaraines in boat-conformers **2b–d** are less planar because this minimizes steric strain and maximizes attractive cross-component attractions. In some of the X-ray structures there are close intra- and intermolecular distances between certain atoms in the surrounding macrocycle and the terminal stopper groups on the encapsulated dye, but there does not appear to be any systematic set of close interactions that explain the switch of solid-state conformations from chair to boat.

To test the empirical hypothesis that pyridyl-containing macrocycles are more likely to adopt a solid-state boat conformation, we prepared and investigated rotaxane **2e**, which has an isophthalamide-containing macrocycle and thus is an analogue of pyridyl-containing **2d**. The X-ray crystal structure of **2e** is shown in Figure 2. The surrounding macrocycle adopts a flattened chair conformation, and the macrocycle is translocated from the center of the encapsulated squaraine. Indeed, the macrocycle conformation in **2e** is intermediate between the chair in **2a** and the boat in **2d**. *It appears, from the crystal structures in hand, that squaraine rotaxanes with pyridyl-containing macrocycles are more likely to adopt macrocyclic boat conformations than rotaxanes with isophthalamide-containing macrocycles, but the solid-state conformations are influenced by crystal packing forces.* In the solution-state, there is no evidence that the macrocyclic boat conformation is predominant for any of the bis(anilino) squaraine rotaxanes **2a–e**. In each case, the ^{1}H NMR spectra indicate that the rotaxane structure is symmetrical on the NMR time scale, and the spectral pattern is essentially unchanged at low temperatures. Specifically, the spectra for **2b** and **2c** in CD$_2$Cl$_2$ were monitored down to −90 °C, where there was slight peak broadening, but little change in chemical shifts. The macrocycles in these symmetrical squaraine rotaxanes are either predominantly in a chair conformation or a rapidly exchanging chair/boat equilibrium. Evidence for the latter stems from the signal pattern for the four equivalent sets of macrocycle methylene protons. The two methylene protons would be diastereotopic if the macrocycle was rigidly fixed in a chair or boat conformation (this feature is observed below with rotaxane **5**), however, both protons have the same chemical shift and they are equally coupled (J = 5.8 Hz) to the adjacent NH residue (Figure 4a). This spectral pattern suggests that the rotaxane macrocycles are rapidly exchanging between different conformations, and that the exchange barrier is quite low. The X-ray structures provide snapshots of the likely intermediates in the co-conformational

exchange process.[12] As the macrocycle flips between the two degenerate chair and two boat conformations, its linear position relative to the center of the squaraine thread undergoes harmonic oscillation (Figure 5). Overall, it appears that the conformational energy landscape for the phenylene-containing tetralactam in these symmetrical squaraine rotaxanes is quite flat, and the different macrocyclic conformations are energetically similar.

The photophysical properties of symmetrical squaraine dyes **1a–d** and their corresponding squaraine rotaxanes **2a–e** are listed in Table 2. Compared to the precursor squaraines, the absorption/emission maxima for rotaxanes **2a–d** with pyridyl-containing macrocycles are red-shifted by about 10 nm while maintaining similar fluorescence quantum yields (0.65–0.72). The isophthalamide-containing macrocycle in squaraine rotaxane **2e** induces a 20 nm red-shift of the absorption/emission maxima and significantly decreases the fluorescence quantum yield to 0.26. The decreased quantum yield seems to be related to the fact that the isophthalamide-containing macrocycle is not wrapped as tightly around the encapsulated squaraine as the pyridyl-containing macrocycle (as listed in Table 1, the centroid-to-centroid distance between the phenylene-sidewalls is 7.16 Å for **2e**, which is substantially longer than the 6.66 Å for analogue **2d**). Squaraine rotaxane **2e** is less rigid and able to undergo dynamic motions that allow radiationless loss of excited state energy.[15]

Truncated Squaraine Rotaxane

The absorption/emission maxima of the symmetrical bis(anilino)squaraine rotaxanes, **2a–e**, match the Cy-5 filter set (approximately 590–635 nm excitation, 650–720 nm emission) that is commonly employed on microscopes and related photonic devices. We have previously shown that these symmetrical squaraine rotaxanes exhibit greatly enhanced stability, and they have tremendous potential as substitutes for the problematic Cy-5 fluorophore in various imaging applications.[16] This success has motivated us to develop other classes of squaraine rotaxanes with altered chromophores that emit at different wavelengths, and here we describe the novel truncated squaraine rotaxane **5** with shorter absorption/emission wavelengths that match the Cy-2 filter set (also known as the FITC filter set, approximately 450–490 nm excitation, 500–550 nm emission).

The synthesis of **5** started with the semisquaraine **3** (Scheme 1), a literature compound that was prepared from squaric acid.[17] Condensation of **3** with *N,N*-dibenzylamine resulted in 1,3-substitution and produced the truncated squaraine dye **4** in 45 % yield.[18] Conversion to the truncated squaraine rotaxane **5** was achieved in 25 % yield by reacting isophthaloyl chloride with 1,4-xylylenediamine in the presence of template **4**. Recrystallization of **5** gave single crystals that were suitable for analysis by X-ray diffraction, and the refined solid-state structure is shown in Figure 6. The unsymmetrical squaraine dye is encapsulated inside a boat-conformation macrocycle that has its two bridging isophthalamide units pointing towards the *N,N*-dibenzyl stopper group at the more distant end of the dye. The intramolecular distances listed for **5** in Table 1 show that the bifurcated hydrogen bonds between the macrocyclic NH residues and the encapsulated squaraine oxygens have normal distances and angles, and the centroid-to-centroid distance between the phenylene-sidewalls is also typical for an isophthalamide-containing macrocycle. Like the other boat-conformer structures described above, the macrocycle is off-set from the squaraine C_4O_2 core.

In CHCl$_3$, the truncated squaraine rotaxane, **5**, rigidly maintains its solid-state macrocyclic boat conformation. This conclusion is based on variable temperature ^{1}H NMR data. In contrast to the single macrocycle methylene peak for rotaxane **2d** (Figure 4a), the methylene protons in **5** are diastereotopic and they have significantly different chemical shifts (Figure 4b). The two inequivalent CH signals exhibit strong geminal coupling ($J = 14.4$ Hz) and unequal vicinal coupling with the adjacent NH residue ($J = 8.2$ Hz versus 1.5 Hz). Furthermore, the splitting pattern does not change over the temperature range +50 °C to −50 °C (see supporting

information), which indicates that the macrocycle conformation is fixed as the boat structure shown in Figure 6.[19,20] It is worth noting that the four aromatic protons on each of the phenylene-sidewalls are chemical shift equivalent, even at −50° C, indicting that both 1,4-phenylene rings are spinning rapidly on the NMR time-frame.

The absorption/emission spectra for truncated squaraine dye **4** and squaraine rotaxane **5** in CHCl$_3$ are shown in Figure 7, and the numerical data are listed in Table 3. As expected for yellow compounds, the dye **4** and rotaxane **5** absorb at 456 nm and 475 nm, respectively, with the rotaxane having a slightly higher molar absorptivity. The emission spectra exhibit a remarkable difference, in that the fluorescence quantum yield of 0.50 for rotaxane **5** is more than four times higher than the value of 0.11 for parent dye **4**. Indeed, squaraine rotaxane **5** is about six times brighter than the parent squaraine **4** (brightness is defined in Table 3). This result is notable and pleasing since one of our major research goals is to develop dye encapsulation strategies that improve the brightness of fluorescent dyes. We propose that the encapsulated squaraine dye in **5** is sterically constrained, and that encapsulation decreases out-of-plane deformations of the *N,N*-dibenzyl nitrogen atom that is attached directly to the squaraine chromophore, and inhibits rotation around the corresponding C-N bond.[15] These effects combine to enhance molar absorptivity and also decrease radiationless decay of the squaraine excited state.

The next characterization step was to determine the relative stabilities of truncated squaraine dye **4** and squaraine rotaxane **5**. To determine photostability, separate cuvettes containing the squaraine **4** or rotaxane **5** in CHCl$_3$ were continuously irradiated using a 150 W xenon arc lamp located 15 cm away, and the absorption was monitored over time. As shown in Figure 8, the absorption decay half-life was approximately 100 seconds for squaraine **4**, and around 1100 seconds for rotaxane **5**, indicating that the latter undergoes a much slower photobleaching process. The photoprotection is similar in magnitude to that observed with previous squaraine rotaxanes.[12a] To determine ground state chemical stability, three separate cuvettes containing the symmetrical bis(anilino)squaraine **1a**, the truncated squaraine **4**, and truncated squaraine rotaxane **5** in CHCl$_3$ (each 10 μM) were treated with a large excess of the 2-mercaptoethanol (50 mM). As shown in Figure 9, the color of the symmetrical squaraine **1a** was lost within ten minutes due to attack of the thiol nucleophile at the electrophilic C$_4$O$_2$ core.[21] In strong contrast, the truncated squaraine **4** and truncated squaraine rotaxane **5** resisted thiol attack and there was no loss of color after 30 minutes. However, the treated cuvette containing dye **4** lost its color over the much longer time frame of one month, whereas the treated cuvette containing **5** was essentially unchanged. We conclude that the C$_4$O$_2$ core of truncated squaraine dye **4** is much less electrophilic than the core of bis(anilino)squaraine **1a**, because the electron releasing effect of the directly attached nitrogen atom in **4** is much stronger than the aromatic aniline in **1a**. Nonetheless, **4** is still susceptible to eventual nucleophilic attack by thiols and it also undergoes photobleaching. Both of these dye degradation processes can be strongly inhibited by permanent encapsulation of the dye as rotaxane **5**.

Conclusions

Permanent encapsulation of bis(anilino)squaraine dyes **1a**–**d** inside Leigh-type tetralactam macrocycles produces squaraine rotaxanes **2a**–**e** that have slightly red-shifted absorption/emission wavelengths, similar or decreased brightness, and substantially enhanced chemical and photochemical stabilities. The surrounding macrocycles are flexible and undergo rapid chair/boat conformational exchange in solution. A series of X-ray crystal structures provide snapshots of several intermediates in the co-conformational exchange process, which involves lateral oscillation of the macrocycle relative to the center of the encapsulated squaraine thread (Figure 5). Pyridyl-containing macrocycles are more likely to adopt boat conformations in the solid-state than analogous squaraine rotaxane systems with isophthalamide-containing

macrocycles. The truncated squaraine dye **4** is less electrophilic than the bis(anilino)squaraine family **1**, but it is still susceptible to chemical and photochemical degradation. Its stability is greatly enhanced when it is converted into truncated squaraine rotaxane **5**. An X-ray crystal structure of **5** shows the macrocycle in a boat conformation (Figure 6) and NMR studies indicate that the boat is maintained in solution. Most notably, mechanical encapsulation of **4** as rotaxane **5** increases the dye's brightness by a factor of six (Table 3). The encapsulation process appears to constrain the dye and reduce deformation of the chromophore from planarity. This study expands our basic understanding of squaraine rotaxane dynamic structure and improves our ability to use mechanical encapsulation as a rational design parameter to fine-tune the chemical and photochemical properties of encapsulated dyes.

Experimental Section

General procedure to synthesize squaraine dyes, 1a–d

The appropriate *N,N*-dibenzyl aniline derivative (1.2 mmol) was added to a solution of 3,4-dihydroxy-3-cyclobutene-1,2-dione (67 mg, 0.59 mmol) in a mixture of benzene (30 mL) and *n*-butanol (15 mL) contained in a 100 mL round bottom flask. The flask was equipped with a Dean-Stark apparatus and refluxed for 16 h. After cooling, the solvent was removed under reduced pressure and the crude product precipitated by washing with hexanes (40 mL). This crude product was purified by column chromatography using a column of silica gel with MeOH/CHCl$_3$ (1:19) as the eluent to give the squaraine dye as a green solid in 30–50 % yield. Spectral data for squaraine **1c**: ^{1}H NMR (300 MHz, CDCl$_3$): δ 4.70 (s, 8H), 6.83 (d, *J* = 9.0 Hz, 4H), 7.05 (d, *J* = 8.7 Hz, 8H), 7.48 (d, *J* = 9.0 Hz, 8H), 8.38 (d, *J* = 9.0 Hz, 4H); ^{13}C NMR (150 MHz, CDCl$_3$): δ 53.8, 113.3, 121.4, 122.0, 128.4, 132.5, 134.0, 134.9, 155.0, 182.9, 192.0; MS (FAB): [*M*]$^+$ 939.9.

Procedure to synthesize truncated squaraine dye, 4

To a solution of *N,N*-dibenzyl semi-squaraine **3** (400 mg, 1.1 mmol),[17] in isopropyl alcohol (30 mL), *N,N*-dibenzylamine (210 mg, 1.1 mmol) was added. After addition of tri-*n*-butyl orthoformate (1 mL), the reaction was heated to reflux for 12 h. The solvent was removed by rotary evaporation, and the crude product purified by column chromatography using a column of silica gel with CH$_2$Cl$_2$ as eluent to give **4** as a yellow solid in 45 % yield: ^{1}H NMR (300 MHz, CDCl$_3$): δ 4.73 (s, 4H), 4.95 (s, 4H), 6.78 (d, *J* = 9.0 Hz, 2H), 7.20–7.34 (m, 20H), 8.20 (d, *J* = 9.0 Hz, 2H); ^{13}C NMR data was not acquired because of poor solubility; HRMS (FAB): calcd for C$_{38}$H$_{32}$N$_2$O$_2$ [*M* + H]$^+$ 549.2542, found 549.2569.

General procedure to synthesize squaraine rotaxanes 2a–e and 5

Clear solutions of the corresponding diacid chloride (0.31 mmol) and 1,4-xylylenediamine (42 mg, 0.31 mmol) in anhydrous chloroform (5 mL) were drawn into two separate 10 mL syringes. Over 5 h these solutions were added dropwise, using a mechanical syringe pump, to a stirred solution containing the corresponding squaraine dye (0.07 mmol) and triethylamine (71 mg, 0.72 mmol) in anhydrous chloroform (40 mL). After stirring overnight, the reaction was filtered through a pad of Celite to remove any polymeric material. The solvent was removed by rotary evaporation, and the crude product purified by column chromatography using a column of silica gel with MeOH/CHCl$_3$ (1:19) as the eluent to give squaraine rotaxane in 26–40 % yield. Spectral data for rotaxane **2c**: ^{1}H NMR (500 MHz, CDCl$_3$): δ 4.50 (d, *J* = 6.0 Hz, 8H), 4.58 (s, 8H), 6.21 (d, *J* = 9.0 Hz, 4H), 6.54 (s, 8H), 6.97 (d, *J* = 7.8 Hz, 8H), 7.53 (d, *J* = 7.8 Hz, 8H), 7.98 (t, *J* = 7.6 Hz, 2H), 8.10 (d, *J* = 8.4 Hz, 4H), 8.39 (d, *J* =10.5 Hz, 4H), 9.83 (t, *J* = 5.1 Hz, 4H); ^{13}C NMR (125 MHz, CDCl$_3$): δ 43.4, 54.0, 112.6, 120.4, 122.4, 125.4, 128.3, 129.1, 132.6, 134.1, 134.5, 137.0, 138.8, 149.5, 155.0, 163.6, 184.8, 188.0; MS (FAB): [*M*]$^+$ 1472.2.

Supplementary Material

Refer to Web version on PubMed Central for supplementary material.

Acknowledgments

References

1. (a) Rescifina A, Zagni C, Iannazzo D, Merino P. Curr Org Chem 2009;13:448–481. (b) Kay RE, Leigh DA. Pure Appl Chem 2008;80:17–29. (c) Griffiths KE, Stoddart JF. Pure Appl Chem 2008;80:485–506. (d) Kay ER, Leigh DA, Zerbetto F. Angew Chem Int Ed 2007;46:72–191. (e) Loeb SJ. Chem Soc Rev 2007;36:226–235. [PubMed: 17264925] (f) Tian H, Wang QC. Chem Soc Rev 2006;35:361–374. [PubMed: 16565753] (g) Schalley CA, Weilandt T, Bruggemann J, Vögtle F. Top Curr Chem 2005;248:141–200.

2. (a) Yoon I, Miljanic OS, Benitez D, Khan SI, Stoddart JF. Chem Comm 2008:4561–4563. [PubMed: 18815683] (b) Miljanic OS, Dichtel WR, Khan SI, Mortezaei S, Heath JR, Stoddart JF. J Am Chem Soc 2007;129:8236–8246. [PubMed: 17559213]

3. (a) Rijs AM, Compagnon I, Oomens J, Hannam JS, Leigh DA, Buma WJ. J Am Chem Soc 2009;131:2428. [PubMed: 19199633] (b) Larsen OFA, Bodis P, Buma WJ, Hannam JS, Leigh DA, Woutersen S. Proc Natl Acad Sci USA 2005;102:13378–13382. [PubMed: 16150716]

4. (a) Betancourt JE, Martin-Hidalgo M, Gubala V, Rivera JM. J Am Chem Soc 2009;131:3186–3188. (b) Zhu SS, Nieger M, Daniels J, Felder T, Kossev I, Schmidt T, Sokolowski M, Vogtle F, Schalley CA. Chem Eur J 2009;15:5040–5046. (c) Pons M, Millet O. Prog Nucl Magn Reson Spectrosc 2001;38:267–324.

5. (a) Leigh DA, Murphy A, Smart JP, Slawin AMZ. Angew Chem Int Ed 1997;36:728–732. (b) Gatti FG, Leigh DA, Nepogodiev SA, Slawin AMZ, Teat SJ, Wong JKY. J Am Chem Soc 2001;123:5983–5989. [PubMed: 11414832] (c) Lane AS, Leigh DA, Murphy A. J Am Chem Soc 1997;119:11092–11093. (d) Clegg W, Gimenez-Saiz C, Leigh DA, Murphy A, Slawin AMZ, Teat SJ. J Am Chem Soc 1999;121:4124–4129.

6. Brancato G, Coutrot F, Leigh DA, Murphy A, Wong JKY, Zerbetto F. Proc Natl Acad Sci USA 2002;99:4967–4971. [PubMed: 11959948]

7. (a) Alvarez-Perez M, Goldup SM, Leigh DA, Slawin AMZ. J Am Chem Soc 2008;130:1836–1838. [PubMed: 18201092] (b) Barrell MJ, Leigh DA, Lusby PJ, Slawin AMZ. Angew Chem Int Ed 2008;47:8036–8039. (c) Serreli V, Lee CF, Kay ER, Leigh DA. Nature 2007;445:523–527. [PubMed: 17268466] (d) Marlin DS, Cabrera DG, Leigh DA, Slawin AMZ. Angew Chem Int Ed 2006;45:77–83. (e) Biscarini F, Cavallini M, Leigh DA, Leon S, Teat SJ, Wong JKY, Zerbetto F. J Am Chem Soc 2002;124:225–233. [PubMed: 11782174] (f) Asakawa M, Brancato G, Fanti M, Leigh DA, Shimizu T, Slawin AMZ, Wong JKY, Zerbetto F, Zhang SW. J Am Chem Soc 2002;124:2939–2950. [PubMed: 11902885] (g) Brouwer AM, Frochot C, Gatti FG, Leigh DA, Mottier L, Paolucci F, Roffia S, Wurpel GWH. Science 2001;291:2124–2128. [PubMed: 11251112]

8. (a) Caldwell ST, Cooke G, Fitzpatrick B, Long D, Rabani G, Rotello VM. Chem Commun 2008:5912–5914. (b) Zhou W, Chen D, Li J, Xu J, Lv J, Liu H, Li Y. Org Lett 2007;9:3929–3932. [PubMed: 17803314] (c) Zhou W, Chen D, Jialiang X, Lv J, Liu H, Li Y. Org Lett 2007;9:3929–3932. [PubMed: 17803314] (d) Mateo-Alonso A, Brough P, Prato M. Chem Commun 2007:1412–1414. (e) Cooke G, Garety JF, Jordan B, Kryvokhyzha N, Parkin A, Rabani G, Rotello VM. Org Lett 2006;8:2297–2300. [PubMed: 16706510] (f) Li Y, Li H, Li Y, Liu H, Wang S, He X, Wang N, Zhu D. Org Lett 2005;7:4835–4838. [PubMed: 16235901] (f) Onagi H, Rebek J. Chem Commun 2005:4604–4606. (g) Chen L, Zhao X, Chen Y, Zhao CX, Li ZT. J Org Chem 2003;68:2704–2712. [PubMed: 12662041]

9. (a) Mateo-Alonso A, Iliopoulos K, Couris S, Prato M. J Am Chem Soc 2008;130:1534–1535. [PubMed: 18189396] (b) Jagesar DC, Hartl F, Buma WJ, Brouwer AM. Chem Eur J 2008;14:1935–1946. (c) Mateo-Alonso A, Guldi DM, Paolucci F, Prato M. Angew Chem Int Ed 2007;46:8120–8126. (d) Mateo-Alonso A, Fioravanti G, Marcaccio M, Paolucci F, Rahman GMA, Ehli C, Guldi DM, Prato M. Chem Commun 2007:1945–1947. (e) Mateo-Alonso A, Ehli C, Rahman GMA, Guldi DM,

Fioravanti G, Maraccio M, Paolucci F, Prato M. Angew Chem Int Ed 2007;46:3521–3525. (f) Mateo-Alonso A, Fioravanti G, Marcaccio M, Paolucci F, Jagesar DC, Brouwer AM, Prato M. Org Lett 2006;22:5173–5176. [PubMed: 17048871]

10. For other examples of macrocycle conformational equilibria, see: (a) Abbenante G, Fairlie DP, Gahan LR, Hanson GR, Pierens GK, van den Brenk AL. J Am Chem Soc 1996;118:10384–10388. (b) Kumar S, Hundal MS, Hundal G, Kaur N, Singh H. Tetrahedron 1997;53:10841–10850. (c) Loeb SJ, Tiburcio J, Vella SJ. Chem Commun 2006:1598–1600.

11. (a) Arunkumar E, Forbes CC, Noll BC, Smith BD. J Am Chem Soc 2005;127:3288–3289. [PubMed: 15755140] (b) Arunkumar E, Fu N, Smith BD. Chem Eur J 2006;12:4684–4690. (c) Arunkumar E, Sudeep PK, Kamat PV, Noll BC, Smith BD. New J Chem 2007;31:677–683.

12. In this paper we use the term "conformation" when we refer to the macrocycle as an isolated structural entity, and we use the term "co-conformation" when we refer to the entire rotaxane. Co-conformation refers to the relative positions and orientations of the mechanically interlocked components with respect to each other. Fyfe MCT, Glink PT, Menzer S, Stoddart JF, White AJP, Williams DJ. Angew Chem, Int Ed 1997;36:2068–2069.

13. (a) Schalley CA. J Phys Org Chem 2004;17:967–972. (b) Affeld A, Hübner GM, Seel C, Schalley CA. Eur J Org Chem 2001;25:2877–2890. and references therein.

14. The repulsive effect of the pyridyl nitrogen with oxygen-containing guests has been noted before, see: Chang SY, Kim HS, Chang KJ, Jeong KS. Org Lett 2004;6:181–184. [PubMed: 14723523]

15. Jacquemin D, Perpete EA, Laurent AD, Assfeld X, Adamo C. Phys Chem Chem Phys 2009;11:1258–1262. [PubMed: 19209370]

16. Johnson JR, Fu N, Arunkumar E, Leevy WM, Gammon ST, Worms WP, Smith BD. Angew Chem Int Ed 2007;46:5528–5531.

17. (a) Gassensmith JJ, Arunkumar E, Barr L, Baumes JM, DiVittorio KM, Johnson JR, Noll BC, Smith BD. J Am Chem Soc 2007;129:15054–15059. [PubMed: 17994746] (b) Keil D, Hartmann H. Dyes Pigm 2001;49:161–179.

18. Nucleophilic substitution of squaric acid, or its corresponding diesters, with amines can potentially give 1,2- or 1,3-bis(squaramide) isomers as products. The isomer ratio is dependent on the reaction conditions. For discussions of this synthetic chemistry, see: (a) Neuse EW, Green BR. J Org Chem 1974;39:3881–3887. (b) Ramalingam V, Bhagirath N, Muthyala RS. J Org Chem 2007;72:3976–3979. [PubMed: 17419651]

19. The unequal vicinal coupling indicates that the macrocycle is not flipping rapidly on the NMR time-scale between conformations that exchange psuedoaxial and psuedoequatorial CH positions. A fixed macrocyclic chair conformation in 5 can be ruled out because it would exhibit *four* diastereotopic methylene CH signals, corresponding to two sets of inequivalent psuedoequatorial protons and two sets of inequivalent psuedoaxial protons.

20. Because of the planar symmetry in 5 it is not possible to determine by NMR if the surrounding boat conformation macrocycle is pirouetting around the encapsulated squaraine thread. Indeed, it is not trivial to experimentally characterize macrocycle pirouetting for any type of squaraine rotaxane. The squaraine C_4O_2 core has no protons to allow NMR studies, and any NMR observable goup that is directly attached to the core (*e.g.*, an anilino ring) can undergo rapid spinning about the connecting single bond.

21. Ros-Lis JV, Garcia B, Jimenez D, Martinez-Manez R, Sancenon F, Soto J, Gonzalvo F, Valldecabres MC. J Am Chem Soc 2004;126:4064–4065. [PubMed: 15053569]
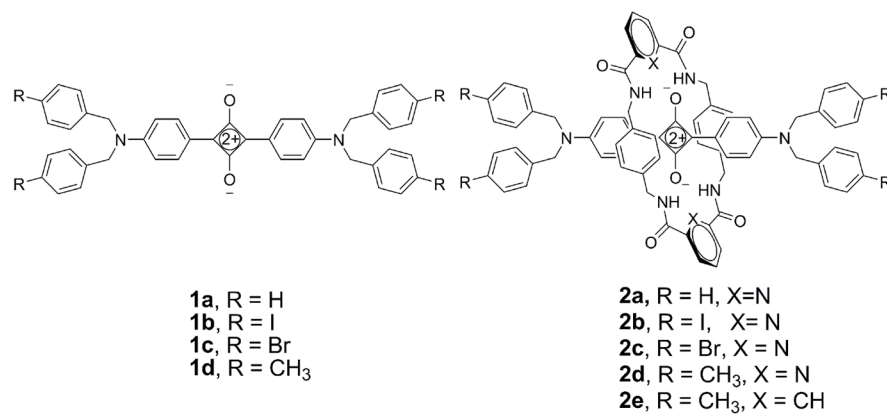
1a, R = H
1b, R = I
1c, R = Br
1d, R = CH₃

2a, R = H, X=N
2b, R = I,   X= N
2c, R = Br, X = N
2d, R = CH₃, X = N
2e, R = CH₃, X = CH

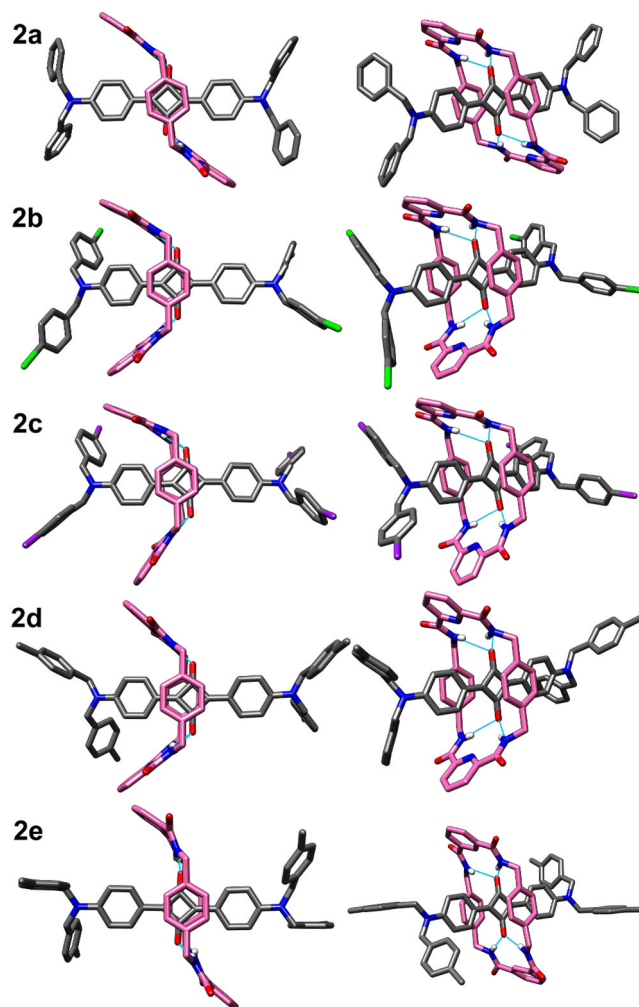**FIGURE 1.**
Squaraine dyes and squaraine rotaxanes.

FIGURE 2.
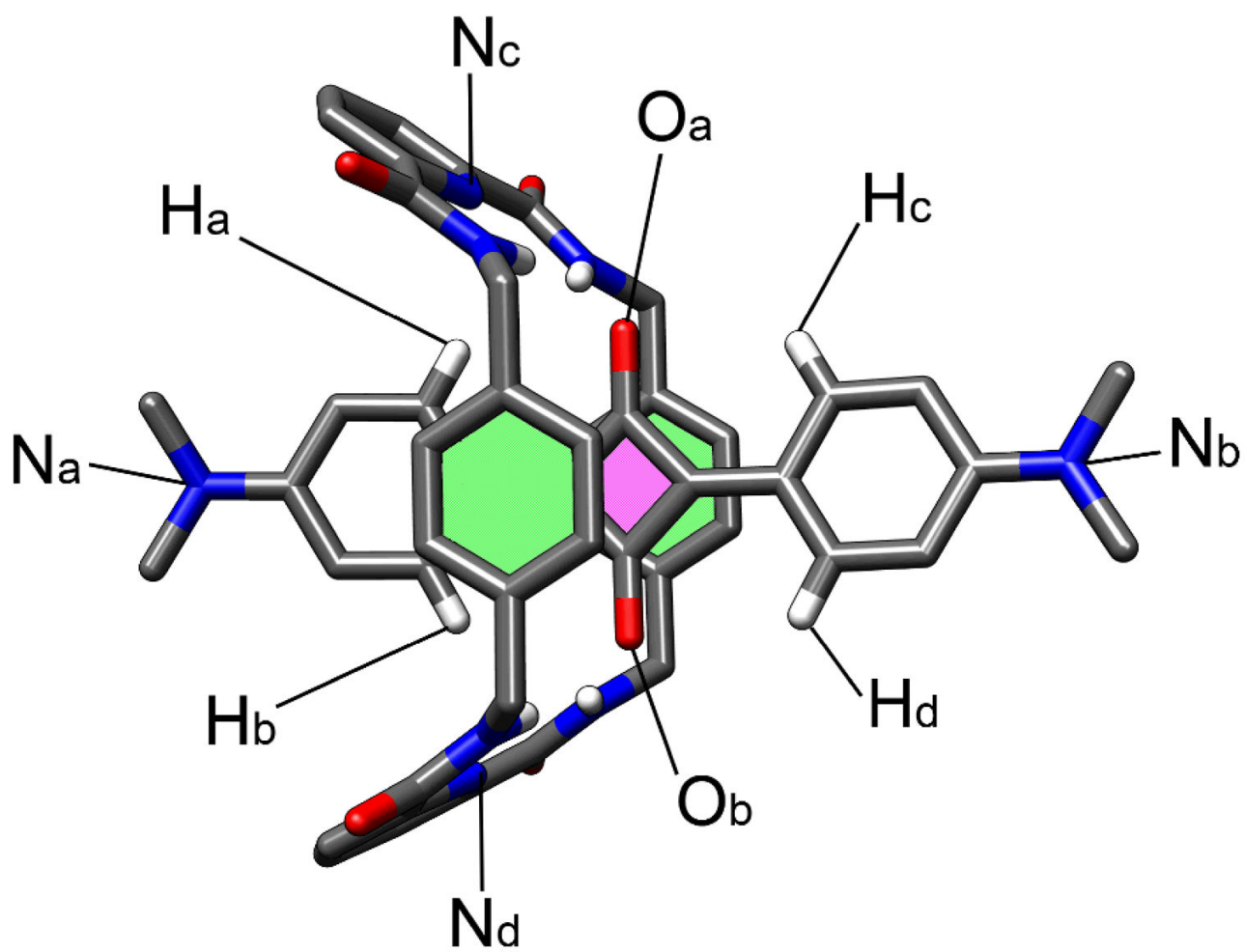X-ray crystal structures of bis(anilino)squaraine rotaxanes **2a–e**.

FIGURE 3.
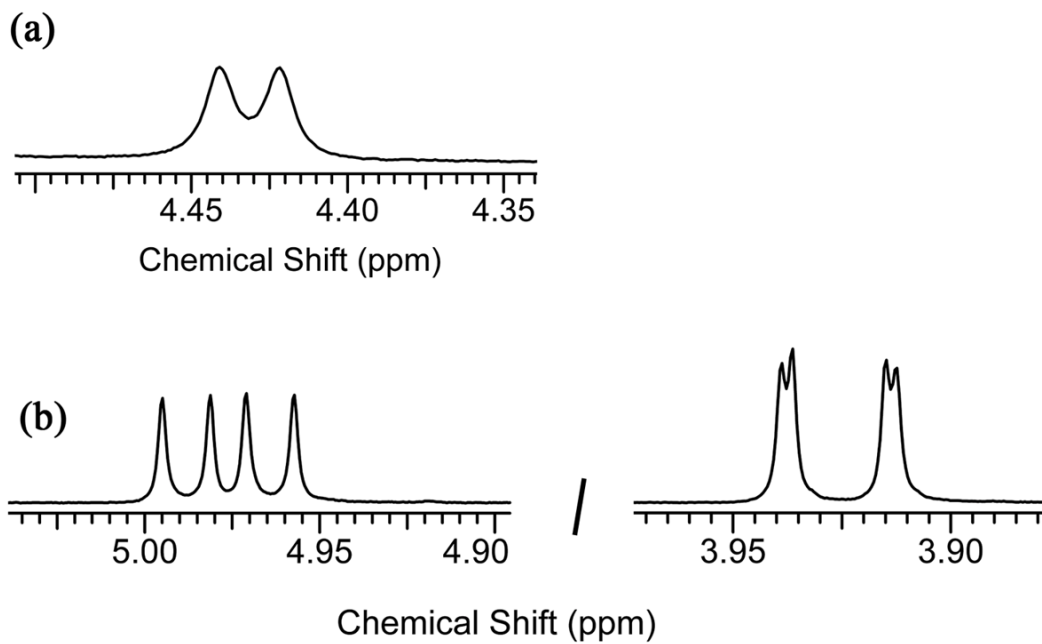Atom labels for squaraine rotaxanes.

FIGURE 4.
Partial ^1H NMR spectra at 22 °C in $CDCl_3$ showing the macrocycle methylene signals for squaraine rotaxanes; (a) **2d** with $J = 5.8$ Hz in a 300 MHz spectrum; (b) **5** with $J_1 = 8.2$ Hz, $J_2 = 14.4$ Hz (left) and $J_1 = 1.5$ Hz, $J_2 = 14.4$ Hz (right) in a 600 MHz spectrum.
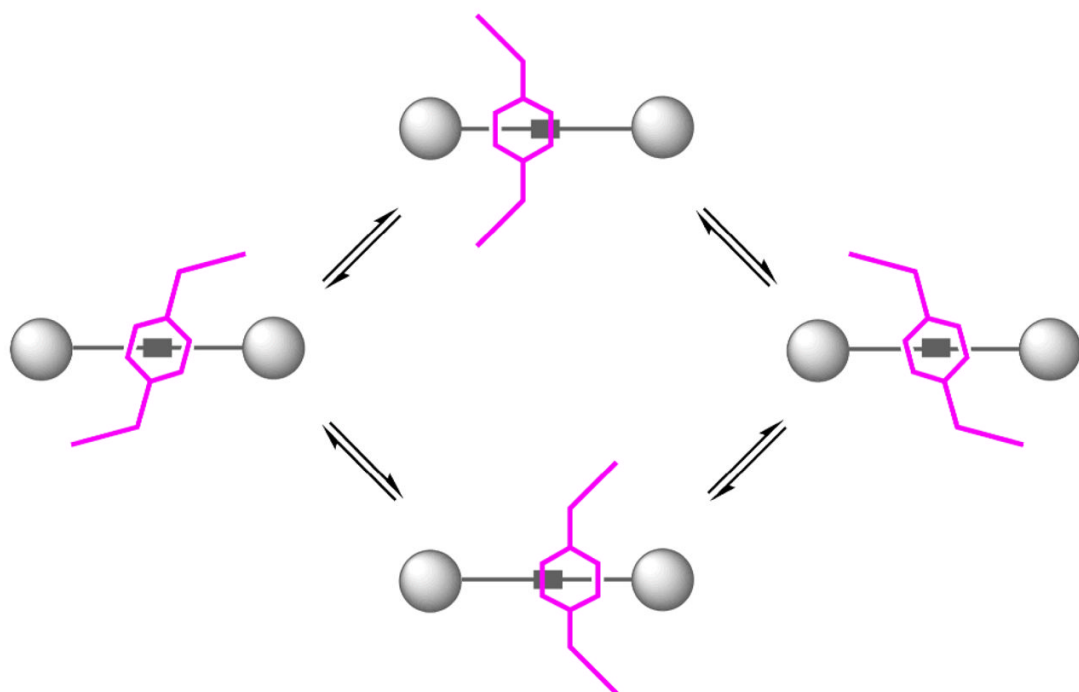
FIGURE 5.
Co-conformational exchange in squaraine rotaxanes **2a**–**e** induces linear oscillation of the macrocycle about the center of the squaraine thread. For clarity, not all possible conformational exchange pathways are shown.
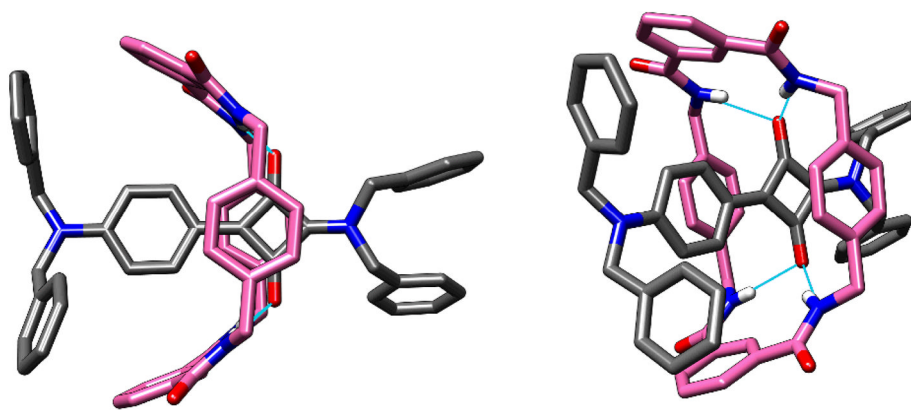
FIGURE 6.
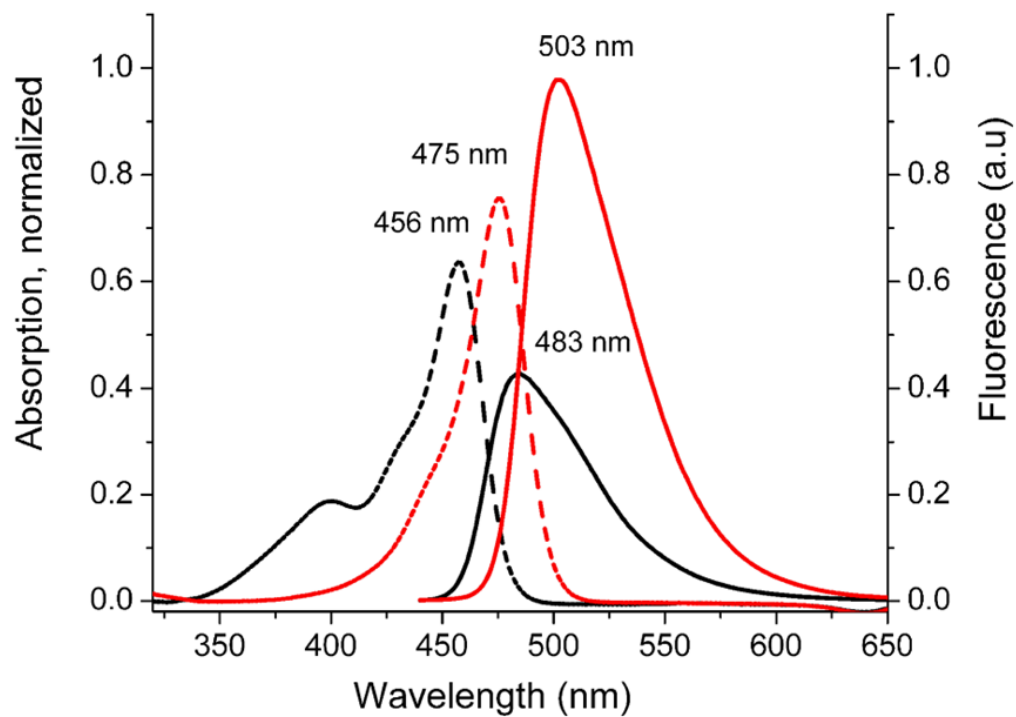X-ray crystal structure of truncated squaraine rotaxane **5**.

FIGURE 7.
Absorption spectra of **4** (– –, black) and **5** (– –, red) and fluorescence emission spectra of **4** (—, black) and **5** (—, red) in CHCl$_3$ (5 μM).
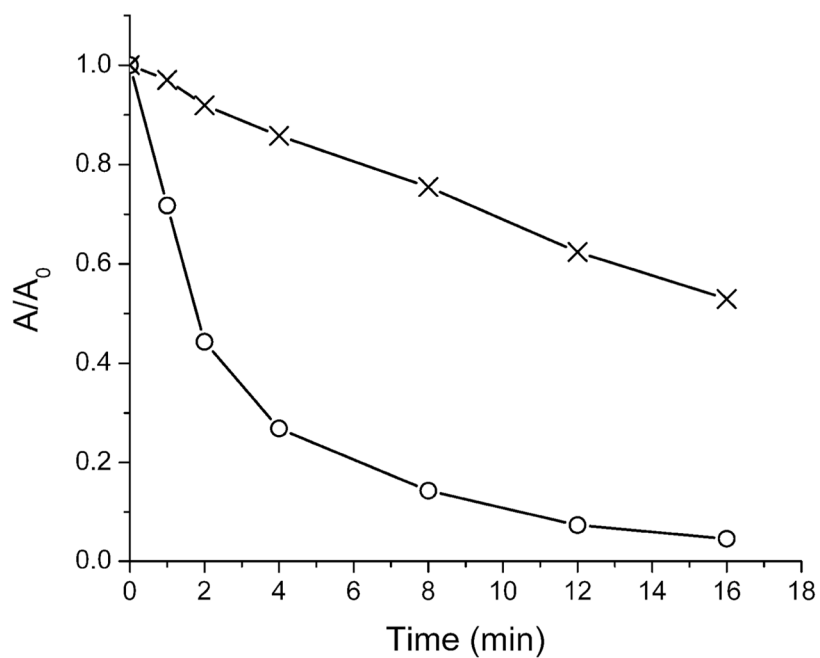
FIGURE 8.
Change in absorption of **4** (○) and **5** (X) in $CHCl_3$ (10 μM) upon exposure to an unfiltered xenon arc lamp (150 W) at 25 °C.
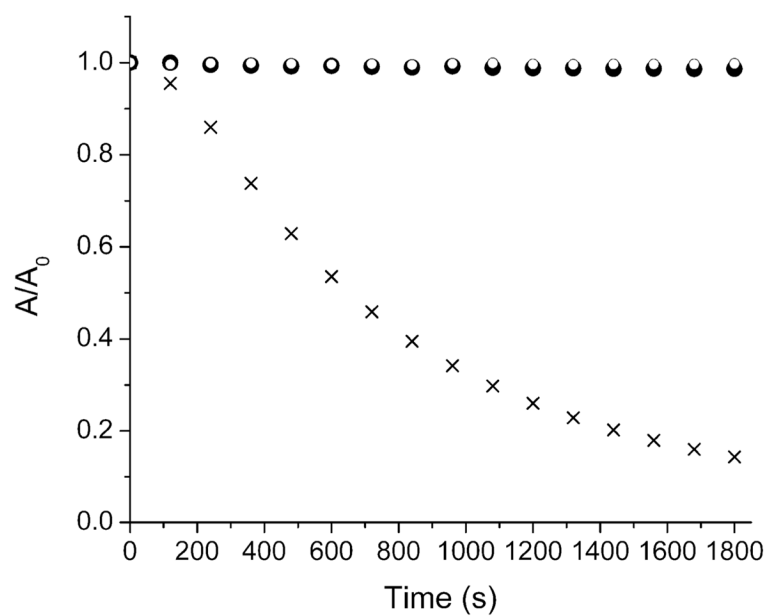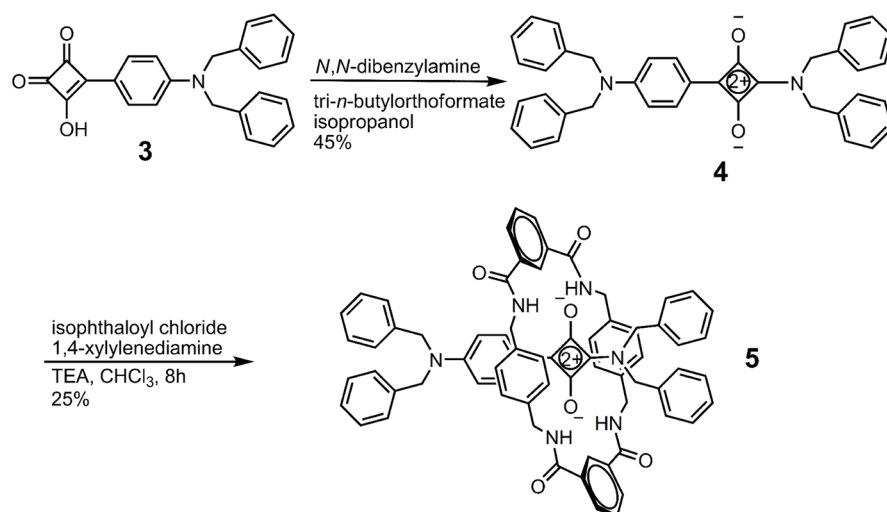
FIGURE 9.
Change in absorption upon addition of 2-mercaptoethanol (50 mM) to **4** (●), **5** (○), and **1a** (X) in $CHCl_3$ (10 μM) at 25 °C.

SCHEME 1.
Synthesis of Truncated Rotaxane 5

TABLE 1

Diagnostic Crystallographic Distances and Angles for Rotaxanes 2a–e and 5

Distance or Angle ^{a}	2a	2b	2c	2d	2e	5
Amide NH•••O (Å)	2.02/2.01	2.13/2.03	2.39/2.39	2.22/2.18	1.95/2.07	2.16/2.18
	2.01/2.01	2.12/2.12	2.14/2.29	2.25/2.04	2.13/2.17	2.15/2.17
Amide N•••H•••O (°)	157.8/156.8	156.3/152.6	146.5/158.2	156.3/153.9	169.4/179.4	163.9/164.0
	156.8/157.8	151.6/151.7	158.7/160.5	156.1/150.1	163.2/146.4	164.0/163.9
Centr.-to-Centr. ^{b} (Å)	6.61	6.63	6.78	6.66	7.16	7.18
N_c-H_a and N_d-H_b (Å)	2.41/2.41 ^{c}	2.41/2.38	2.36/2.53	2.39/2.48	-	-
N_c-O_a and N_d-O_b (Å)	3.15/3.15	3.24/3.32	3.50/3.21	3.35/3.28	-	-
N_a-N_b (Å)	13.29	13.15	13.09	13.16	13.25	-

^{a} Atom labels are in Figure 3.

^{b} Centroid-to-centroid distance between the two parallel 1,4-phenylene sidewalls in the macrocycle

^{c} N_c-H_a and N_d-H_d distances because of chair conformation.

TABLE 2

Photophysical Properties in THF

Compound	λ_{abs} (nm)	$\lambda_{em}{}^a$ (nm)	$\Phi_f{}^b$
1a	631	647	0.70
1b	630	647	0.72
1c	629	648	0.70
1d	632	651	0.65
2a	640	658	0.70
2b	638	657	0.74
2c	636	659	0.67
2d	641	662	0.65
2e	650	674	0.26

[a] Symmtrical dyes **1a–d** and rotaxanes **2a–e** were excited at 580 nm and emission was monitored in the 600–750 nm region for estimating Φ_f.

[b] Fluorescence quantum yields (error limit ± 5 %) were determined for using 4,4-[bis(*N,N*-dimethylamino)phenyl] squaraine dye as the standard (Φ_f = 0.70 in CHCl$_3$) Molar absorptivities were typical of squaraine dyes **1a–d** having log ε = 5.4, squaraine rotaxanes **2a–e** having log ε = 5.6.

TABLE 3

Photophysical Properties in CHCl$_3$

Compound	λ_{abs} (nm)	$\lambda_{em}{}^a$ (nm)	log ε	$\Phi_f{}^b$	Rel. Brightness^c
4	456	483	4.8	0.11	1
5	475	503	4.9	0.50	6

^{a}Short-conjugated squaraine dye **4** and rotaxane **5** were excited at 420 nm and emission was monitored in the 440–650 nm region for estimating Φ_f.

^{b}Using coumarin-6 dye as a standard (Φ_f = 0.78 in ethanol).

^{c}Brightness was determined as molar absorptivity × quantum yield.